Supplementary Information for

Splice Factor Polypyrimidine tract-binding protein 1 (Ptbp1) Primes Endothelial Inflammation in Atherogenic Disturbed Flow Conditions

Corresponding Author
Patrick A. Murphy, Ph.D.
Assistant Professor
Center for Vascular Biology & Calhoun Cardiology Center
University of Connecticut Medical School
263 Farmington Avenue
Farmington, CT 06030
Tel: 860-679-2829
Email : pamurphy@uchc.edu

This PDF file includes:

Figures S1 to S18
Legends for Datasets S1 to S7

Other supplementary materials for this manuscript include the following:

Datasets S1 to S7

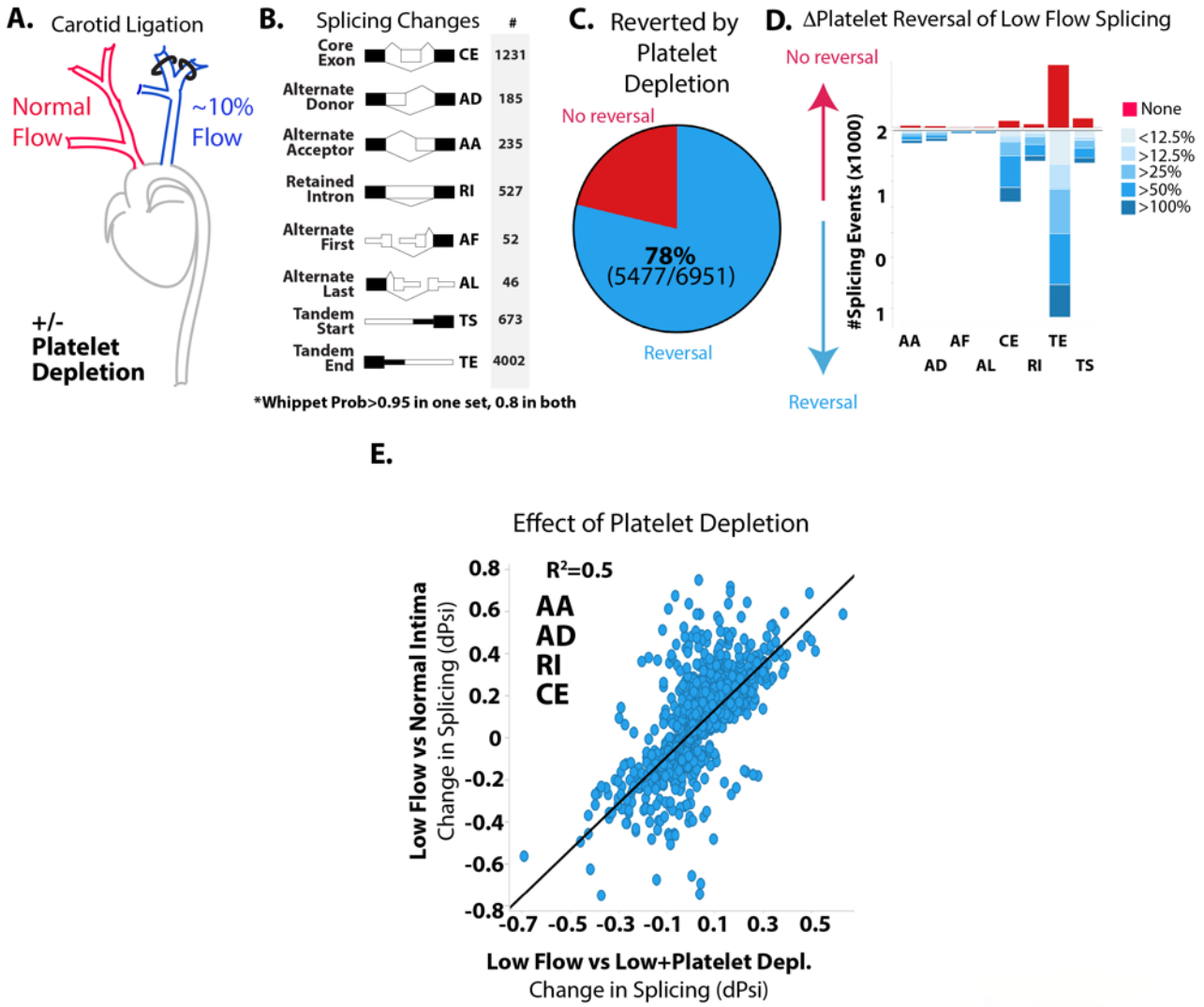

Fig. S1. Platelet depletion reverses splicing changes induced by low and disturbed flow (LDF).
(A) Schematic of approach for RNA splicing responses induced by acute exposure to low and disturbed flow (LDF), (*Murphy et al.* eLife *2018*). Ligation of distal branches of the left carotid artery (blue) leads to a 10% reduction in blood flow. Platelets were depleted by anti-GPIBα treatment at the time of the surgery. (B) Analysis of change in splicing by Whippet analysis. Changes shown represent those with a probability of > 0.95 in one low flow comparison (N=2 v N=2 pools, each pool containing 2-3 arteries), and a probability of at least 0.8 in two biologically independent comparisons of pools. (C&D) Summary of the degree of reversal (or not) with platelet depletion of all splicing events (defined in panel B) induced by LDF for all splicing events (C) and for individual types of splicing events, with a scale to indicate the degree of reversal (D). (E) Graph showing the change in inclusion level (Psi) for the indicated classes of splicing events, in a comparison of LDF versus normal flow intima (y axis) or low flow intima versus low flow intima with platelet depletion (x axis). (F-H) Sashimi plots showing example splicing changes altered under LDF conditions (LF) relative to normal flow conditions (NF) and reverted under LDF conditions after the depletion of platelets (LP_antiplat). In addition, the plots show the effect of adding a combination of platelets and monocytes to endothelial cells *in vitro (*invitro_immune), versus plasma alone (invitro_plasma). Plots are shown in subsequent panels.

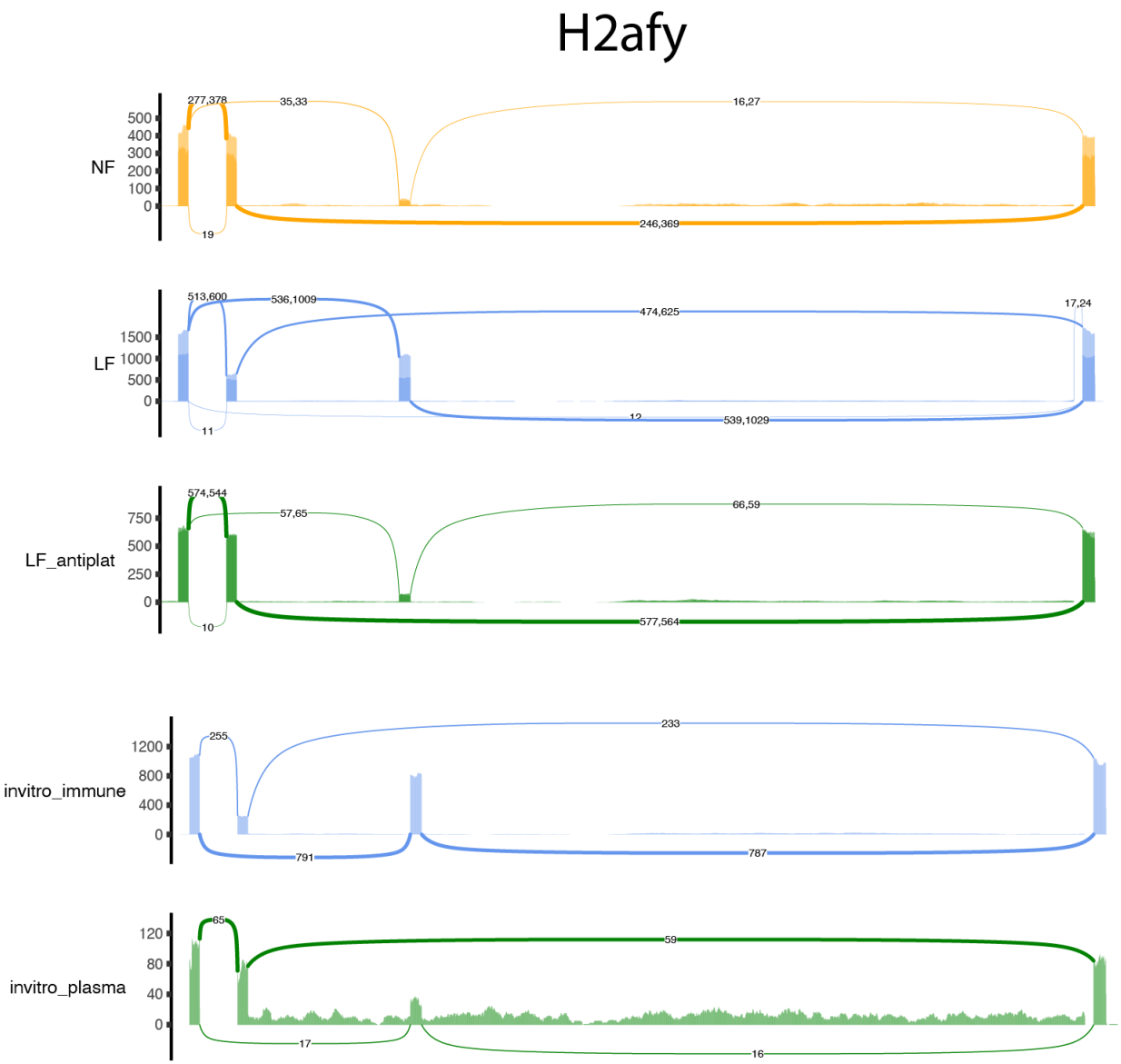

Fig. S1H. Platelet depletion reverses splicing changes induced by low and disturbed flow (LDF). Sashimi plots showing example splicing changes altered under LDF conditions (LF) relative to normal flow conditions (NF) and reverted under LDF conditions after the depletion of platelets (LP_antiplat). In addition, the plots show the effect of adding a combination of platelets and monocytes to endothelial cells *in vitro* (invitro_immune), versus plasma alone (invitro_plasma). Y-axis is read count. Junction reads are indicated above lines between exons. For replicates, these are separated by commas.

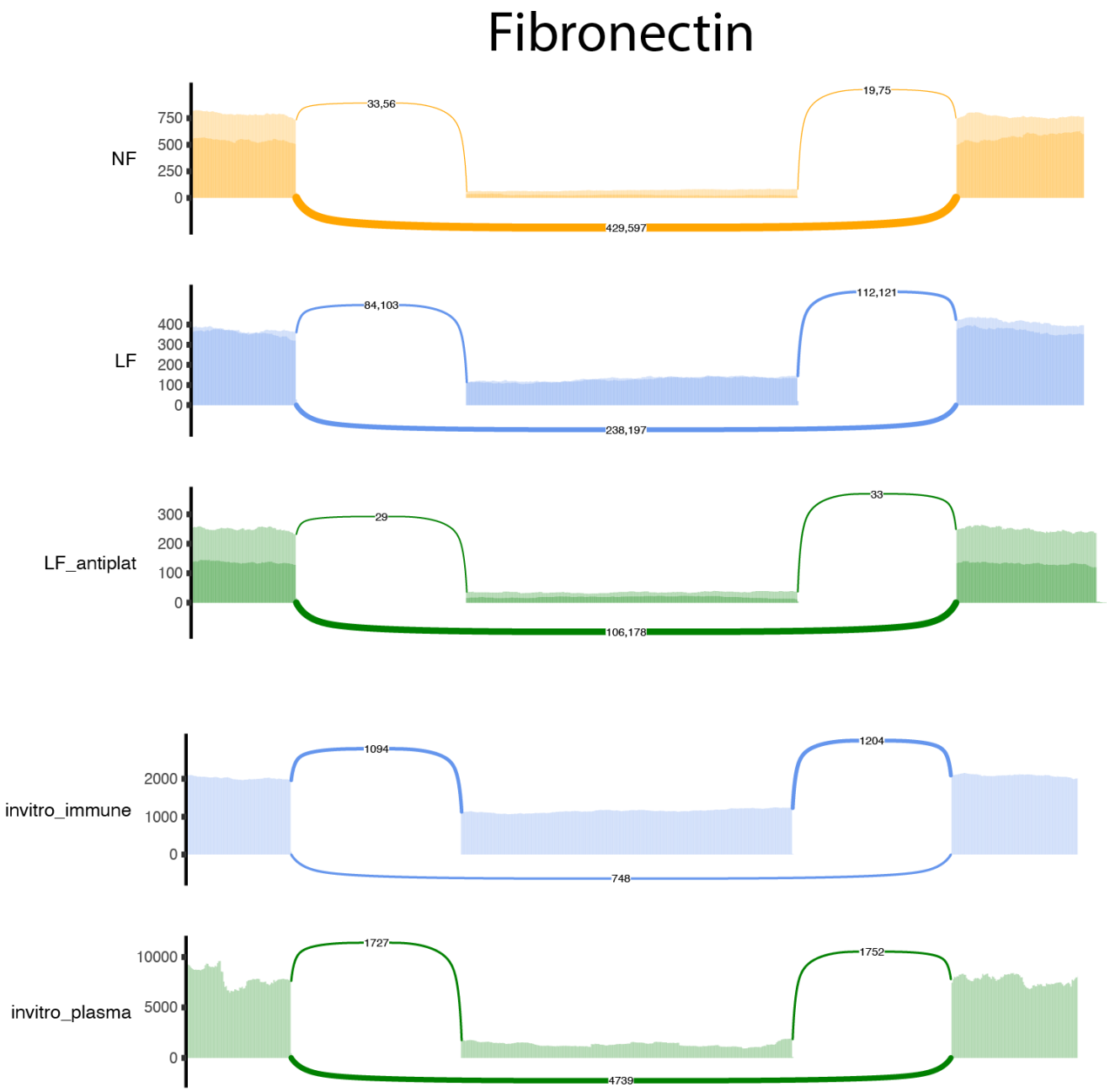

Fig. S1I. Platelet depletion reverses splicing changes induced by low and disturbed flow (LDF). Sashimi plots showing example splicing changes altered under LDF conditions (LF) relative to normal flow conditions (NF) and reverted under LDF conditions after the depletion of platelets (LP_antiplat). In addition, the plots show the effect of adding a combination of platelets and monocytes to endothelial cells *in vitro (*invitro_immune), versus plasma alone (invitro_plasma). Y-axis is read count. Junction reads are indicated above lines between exons. For replicates, these are separated by commas.

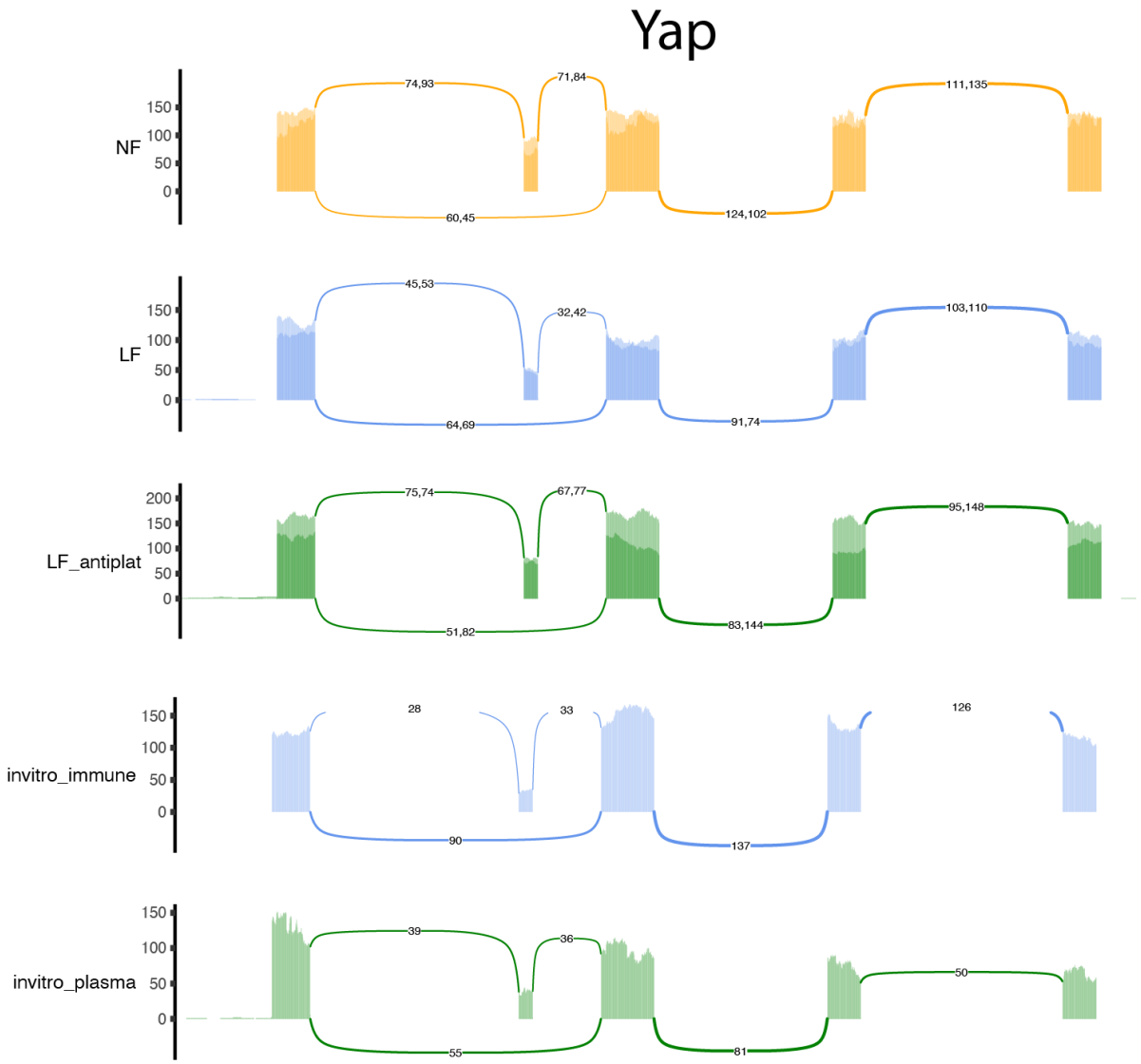

Fig. S1J. Platelet depletion reverses splicing changes induced by low and disturbed flow (LDF). Sashimi plots showing example splicing changes altered under LDF conditions (LF) relative to normal flow conditions (NF) and reverted under LDF conditions after the depletion of platelets (LP_antiplat). In addition, the plots show the effect of adding a combination of platelets and monocytes to endothelial cells *in vitro (*invitro_immune), versus plasma alone (invitro_plasma). Y-axis is read count. Junction reads are indicated above lines between exons. For replicates, these are separated by commas.

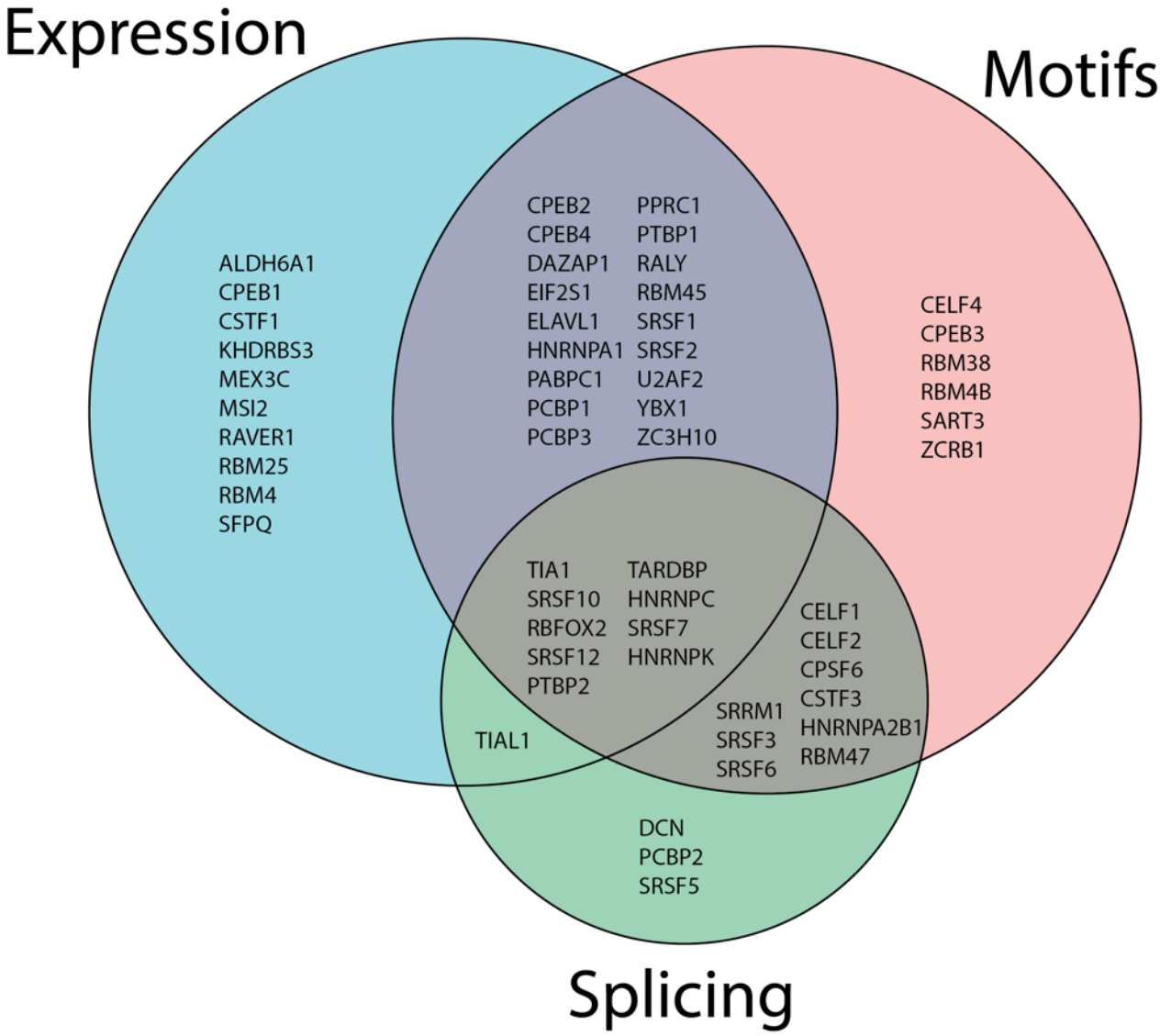

Fig. S2. Characteristics of RNAbp Selected for Targeted CRISPR Screen.
Venn diagram indicating the rationale for the selection of RNAbp in the targeted CRISPR screen. RNAbp selected by expression were altered at the transcript level in the arterial intima in the 48hr or 7day response to low and disturbed flow, or *in vitro* in comparison to quiescent endothelium *in vivo* (Murphy et al., eLife 2018). RNAbp selected by splicing were characterized by altered splicing patterns in the same comparisons (Murphy et al., eLife 2018). RNAbp selected by motifs were linked to enriched motifs nearby skipped exon events regulated in a platelet dependent manner under disturbed flow conditions *in vivo* or *in vitro* (Murphy et al., eLife 2018 and Hensel et al., Sci. Reports 2021).

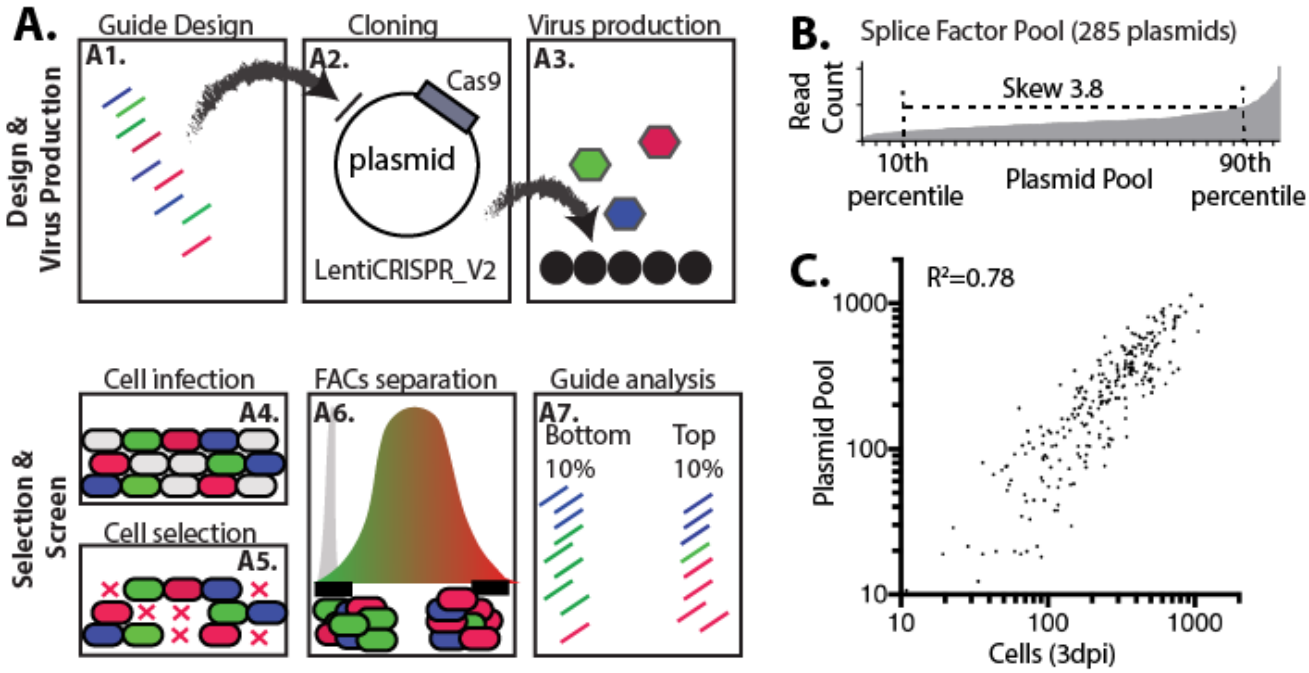

Fig. S3. Showing CRISPR KO screening approach.
(A) Screening approach (A1) Guides to each target gene of interest were designed using the latest rules in the Broad design tool, and as hybridized oligos for (A2) batch cloning into a lentiviral backbone containing Cas9 and guide expression site. (A3) The resultant plasmid library is then used for production of lentivirus and infection of cells (A4). Infection is at 0.3 multiplicity of infection (MOI) and (A5) selection is by puromycin. (A6) Selected cells are sorted on the response to TNFα by ICAM1 and VCAM. Cells in the top 10% and bottom 10% of the response are isolated. (A7) Genomic DNA is isolated and guide enrichment in cells is assessed by sequencing of amplified lentiviral insertions. (B) Read density (y-axis) for each guide construct in the plasmid library for a list of 57 candidate splice factors (5 guides for each gene, x-axis). (C) Plasmid pool is generated as lentivirus and integrated into cells at similar levels. dpi=days post infection.

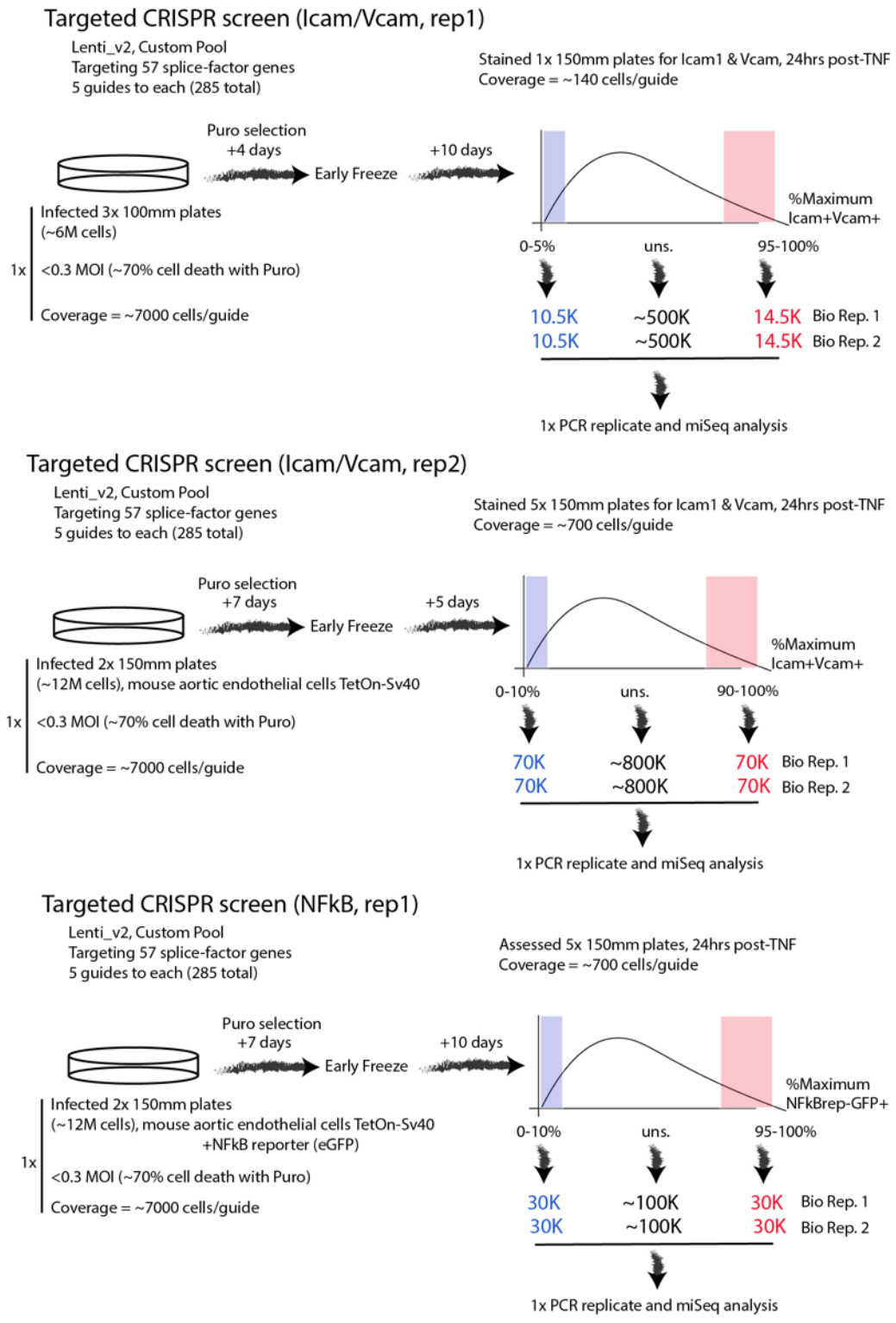

Fig. S4. CRISPR screen coverage.
Schematic showing the preparation and analysis of cells in each individual CRISPR-KO screen performed. Numbers underneath the schematic of the flow-cytometry plot indicate the numbers of sorted cells from the high, low or unsorted fractions used in each biological replicate.

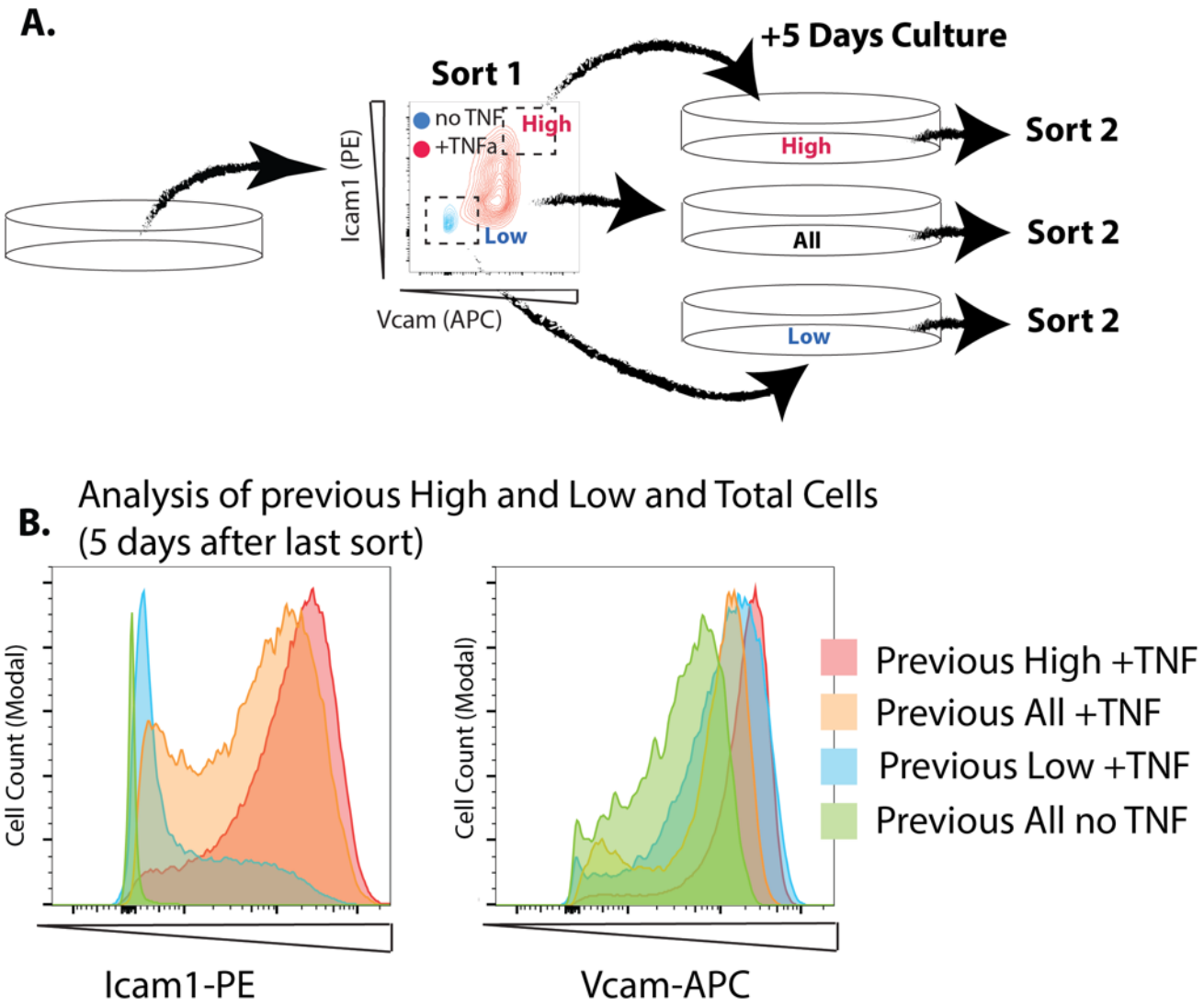

Fig. S5. Retention of Icam/Vcam response in sorted high and low responder populations.
(A) Schematic showing secondary analysis of sorted cells, to confirm that cells which responded with a Low or High response to TNFα treatment initially retained this response upon a second stimulation. Although TNF-treated (red) and untreated (blue) cells are overlaid on the plot, only low and high responders from TNF treated cells were collected and re-assessed 5 days later (B) Modal distribution of previously sorted Icam/Vcam high (High) and Icam/Vcam low (Low) populations, and the total population (All).

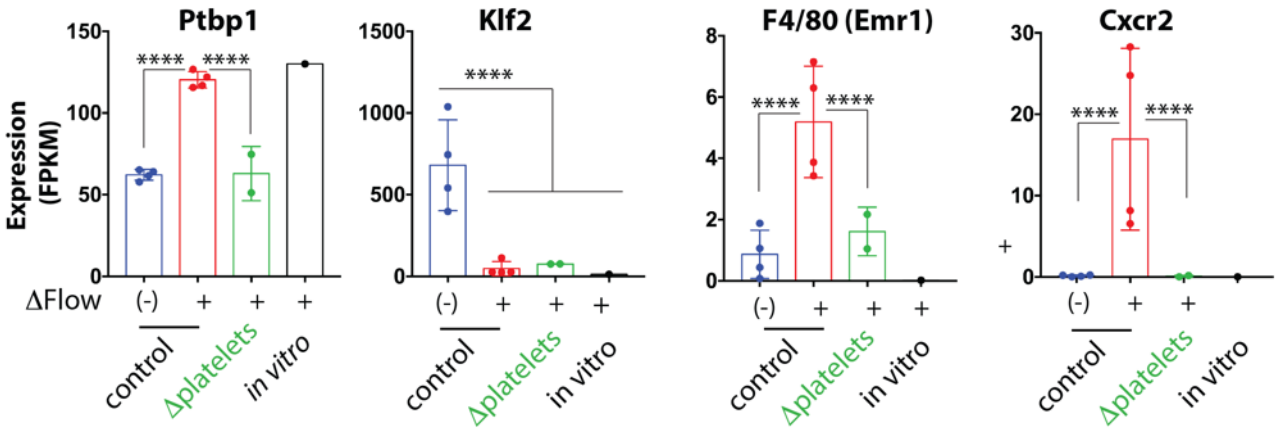

Fig. S6. Analysis of Ptbp1 levels in 48hrs after partial carotid ligation with or without platelet depletion. Re-analysis of RNA-sequencing data from Murphy et al., eLife 2018. Graph showing changes in the levels transcripts from the indicated genes in the carotid intima of vessels exposed to LDF (ΔFlow+), or from vessels exposed to LDF (ΔFlow+) without or with platelet depletion (Δplatelets), or from cultured cells under static *in vitro* conditions (*in vitro*) by RNA-seq analysis. Each point represents a pool of 2-3 arteries. FPKM=Fragments Per Kilobase of transcript per Million mapped reads.

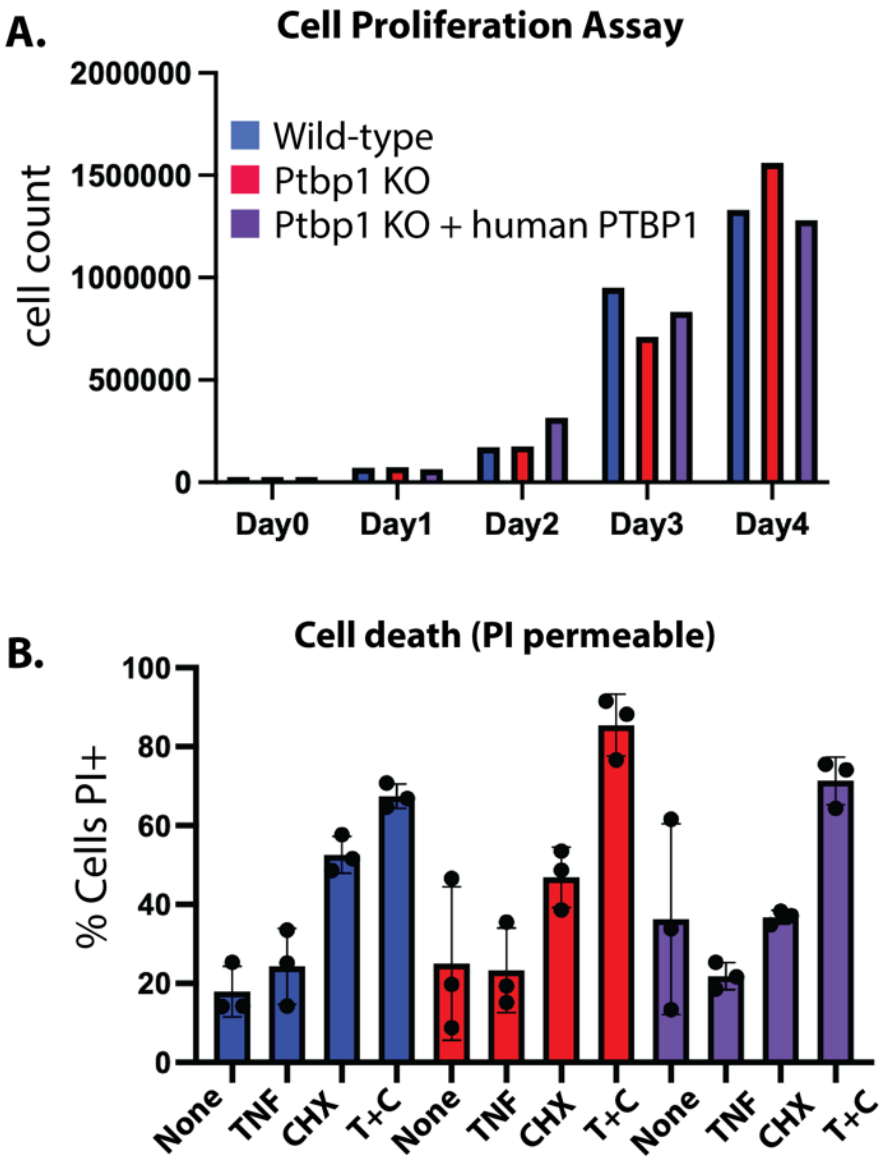

Fig. S7. Ptbp1 deletion effects on proliferation and cell death in response to cytokine and cyclohexamide. (A) Proliferation rates of wild-type aortic endothelial cells (TetOn-Sv40 in 2 µg/mL Dox media) or these cells with Ptbp1 CRISPR-KO, or rescue with human PTPB1 cDNA in the KO cells. (B) Percent of dead cells, positive for propidium iodide, after 24hrs treatment with 100ng/mL TNFa (TNF), 10ug/mL cycloheximide (CHX), or both (T+C).

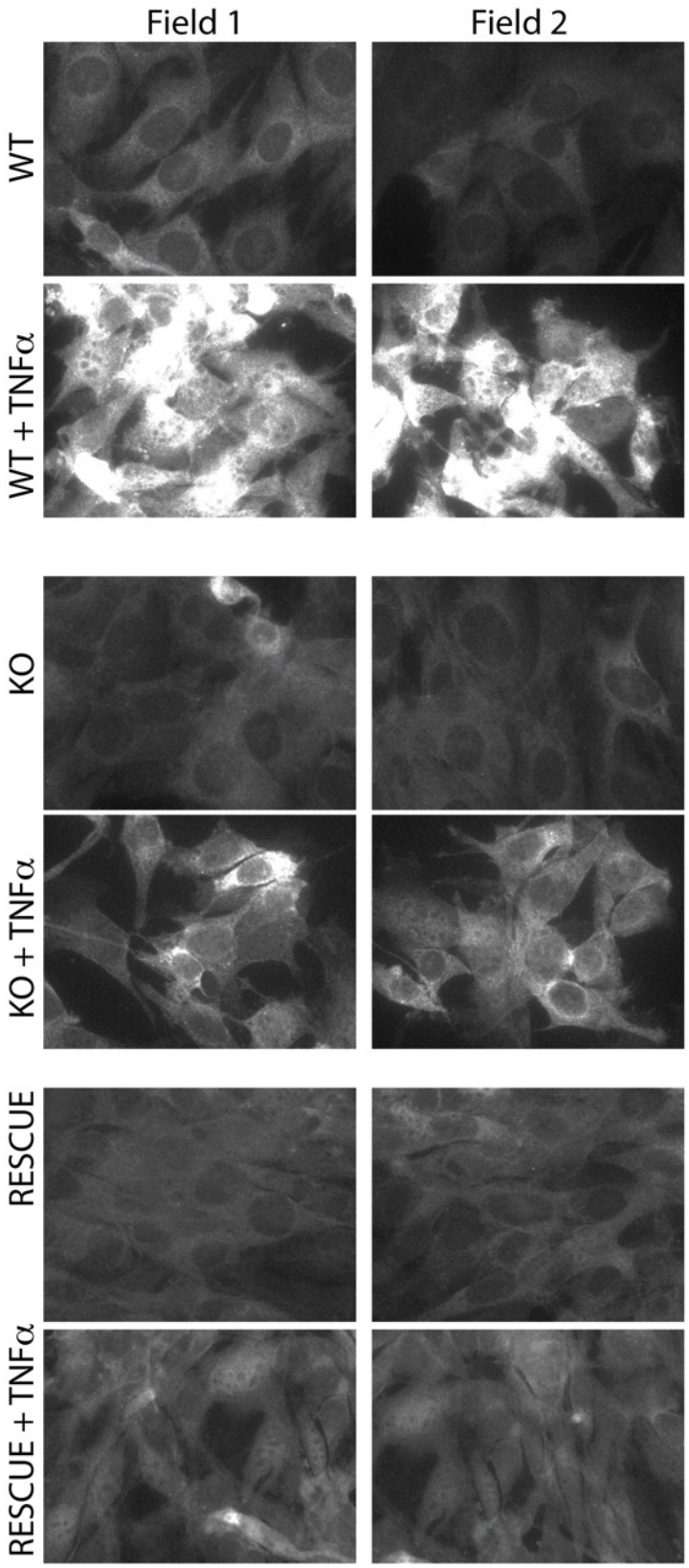

Fig. S8. RelA/p65 localization in cultured aortic endothelial cells.
Immunofluorescence showing the location of RelA/p65 in aortic endothelial cells, and a CRISRP KO clone with deletion of Ptbp1, or rescue with human PTBP1. Images were taken of cells 24hrs after treatment with 30ng/mL TNFα.

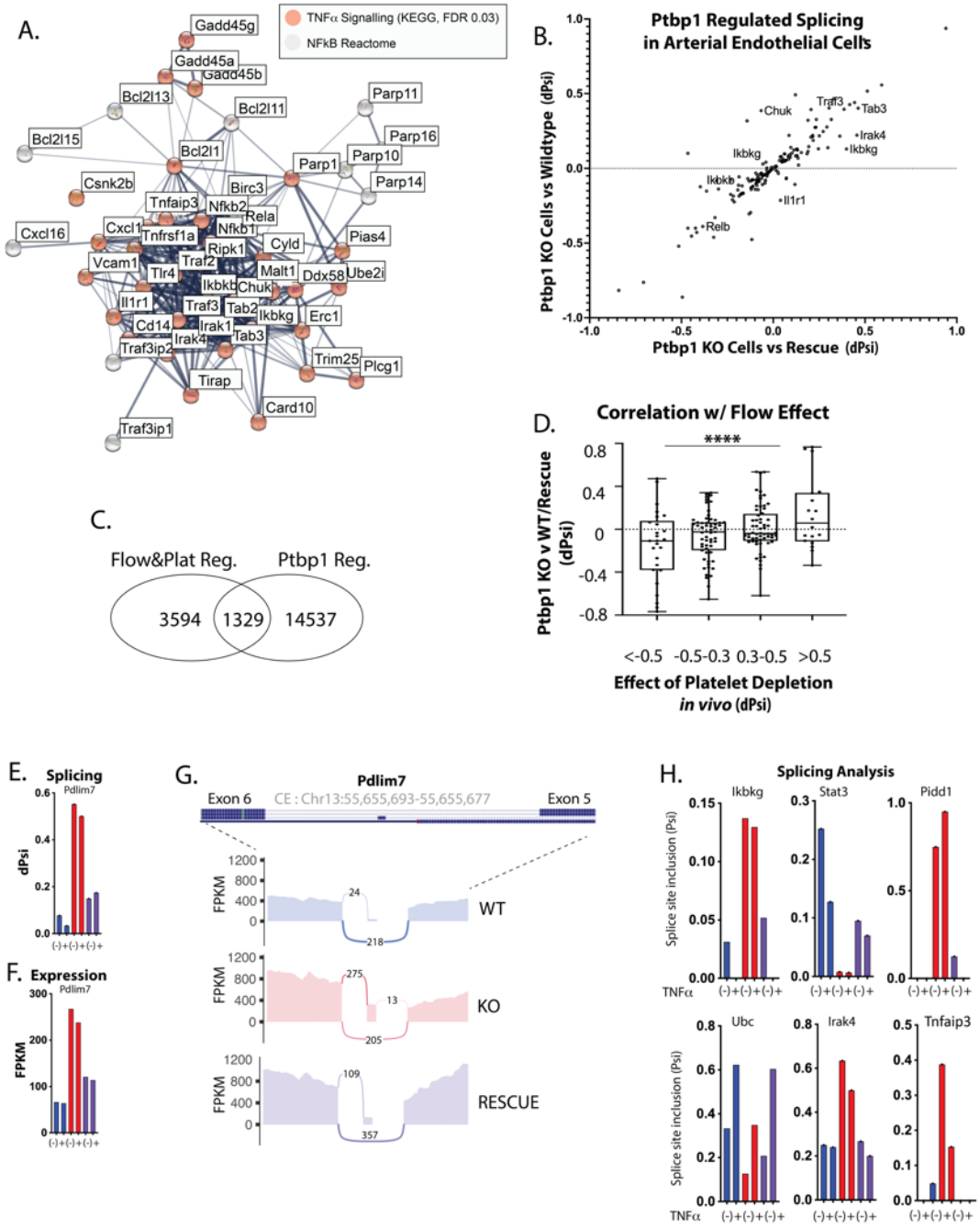

Fig. S9. Ptbp1 regulation of alternative splicing of core NFkB signaling pathway genes and modifiers. (A) String.DB map of protein-protein interactions from genes with Ptbp1 regulated transcripts (Dataset S) – filtered on those in the NFkB signaling pathway (KEGG hsa04064). (B) Correlation between NFkB signaling pathway (KEGG hsa04064) splicing events affected in Ptbp1 CRISPR KO arterial endothelial cells versus control cells (Y-axis) or versus KO cells with Ptbp1 cDNA rescue (X-axis). (C) Venn diagram showing the overlap between the splicing events regulated by platelets in the *in vivo* endothelium and those regulated by Ptbp1 *in vitro* (present in wild-type or rescue cells, but not KO); at least 5 reads were required in all data sets (Probability of 0.8 in three different *in vivo* data sets for platelet regulation, and 0.9 in two different *in vitro* comparisons – all under TNFα treatment, wild-type cells vs Ptbp1 KO, and Ptbp1 KO cells vs Ptbp1 KO cells + human PTBP1 rescue). (D) Analysis of all platelet regulated splicing events, comparing the change in splicing inclusion (Psi) with platelet depletion *in vivo* to the change observed with Ptbp1 deletion *in vitro*. (E-G) Example of alternative splicing (E), transcript level (F) and sashimi plot (G) in one gene altered by both platelets and Ptbp1. (H) Examples of other Ptbp1 regulated splicing events in NFkB regulatory genes.

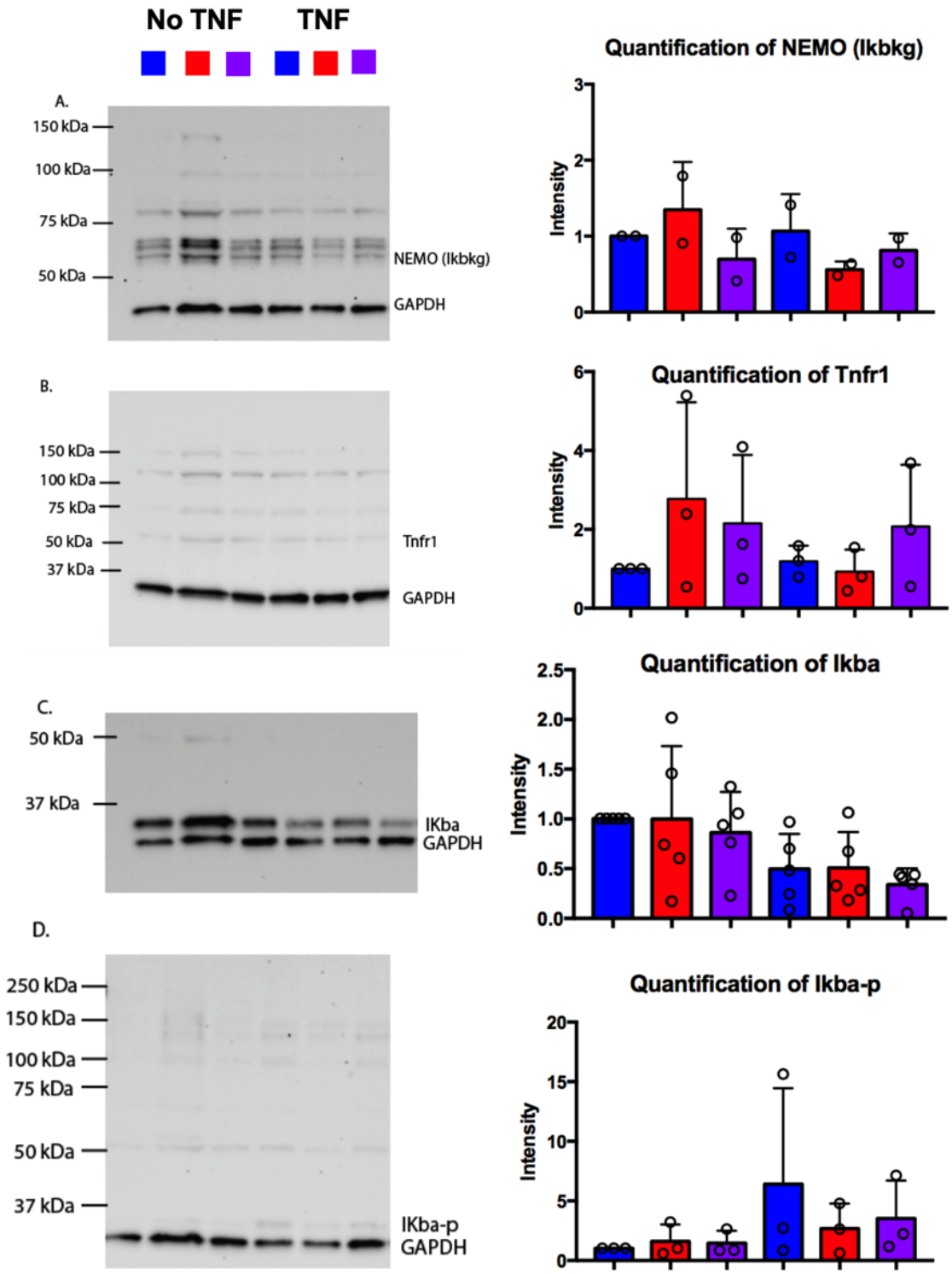

Fig. S10. Analysis of core NFκB pathway components.
(A-D) Western blots and quantitation of signal intensities, relative to GAPDH control from biological replicates of the indicated cell lines (wild-type aortic endothelial cells (blue), Ptbp1 CRISPR-KO (red) and KO with human PTBP1 cDNA (purple), without (left) or with (right) 30ng/mL TNFα.

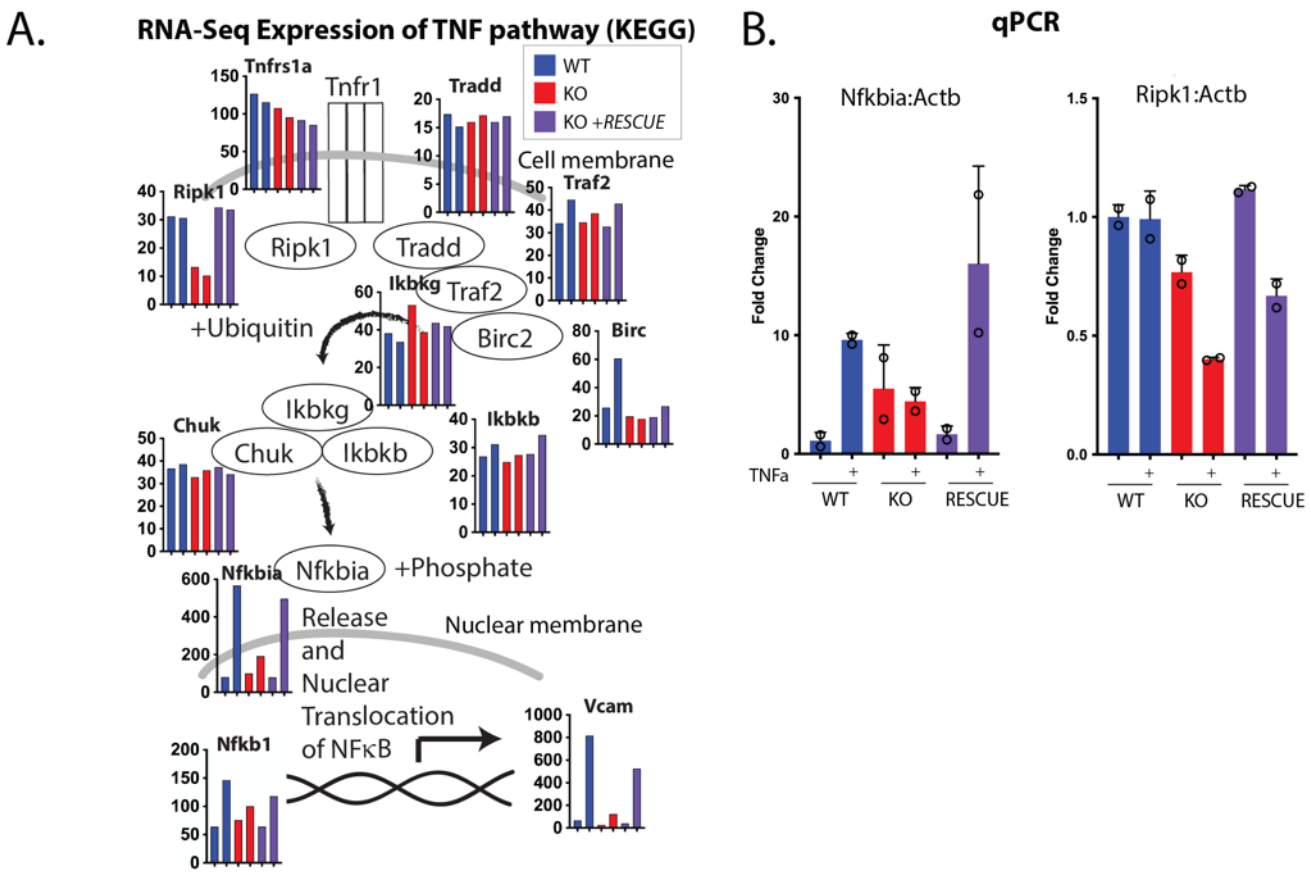

Fig. S11. Ptbp1 regulation of core NFkB pathway transcripts.
(A) Graphs represent TpM (transcripts per million) from RNA sequencing analysis of the cell lines, with and without treatment of TNF. In each graph are, left to right, WT cells without TNFa, and +TNFa, KO cells without TNFa and plus TNFa and Rescue cells without TNFa and +TNFa. (B) Data from qPCR analysis of differential transcripts, showing expression levels normalized to Actb, with the same sample order as outlined in (A), but from a separate set of biological replicates.

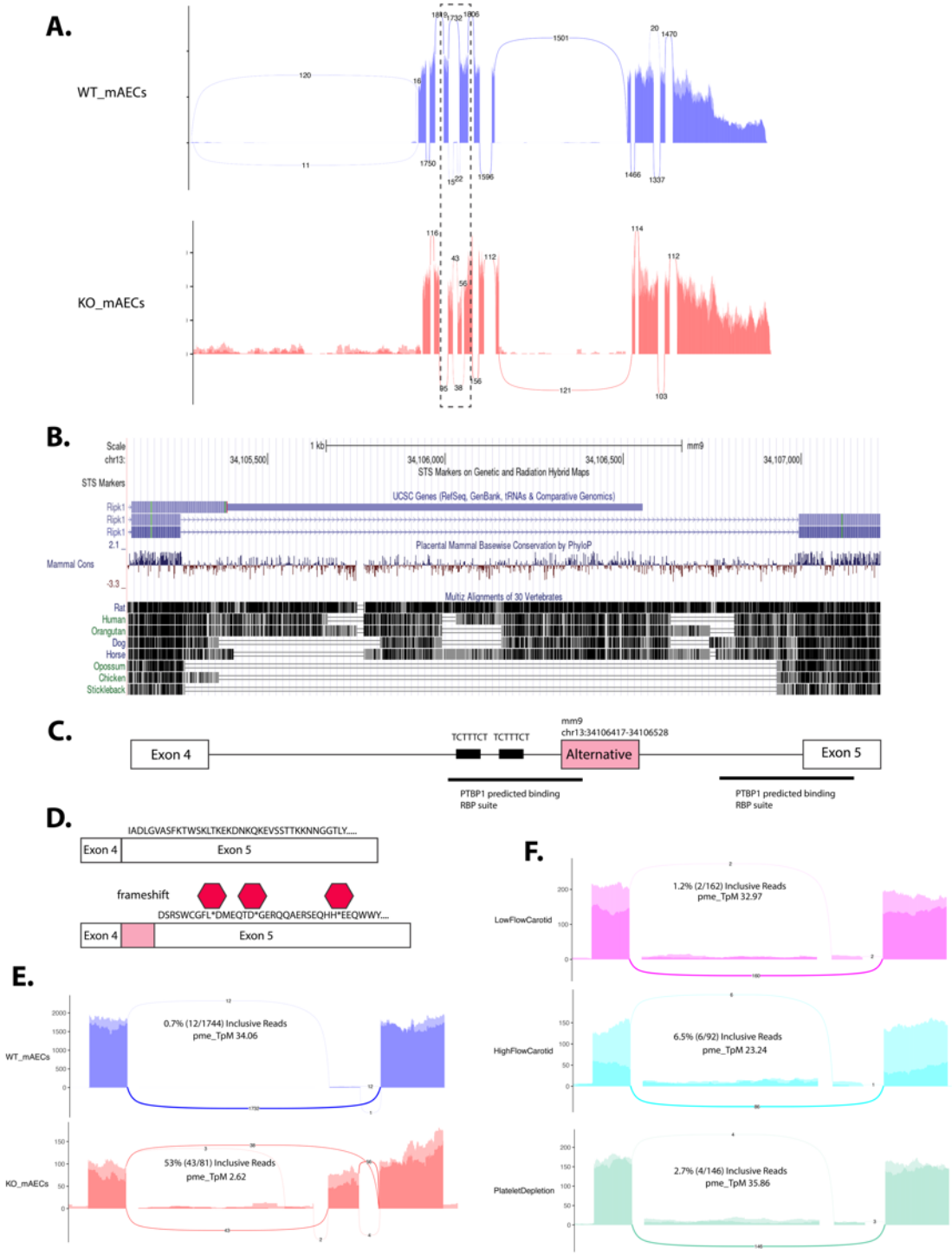

Fig. S12. Ptbp1 suppresses an alternative exon in Ripk1 regulating protein translation.
(A) Sashimi plot, showing full length Ripk1 in primary wild-type and Ptbp1 EC-KO aortic endothelial cells. The dashed area indicated the region of alternative splicing. (B) Track showing mammalian conservation and existing annotations from the UCSC genome browser. (C) Location of high confidence Ptbp1 binding sites by RBP suite, and the location of specific full Ptbp1 motifs. (D) The protein coded by exon 5 with and without inclusion of the alternative exon. Stop signs mark termination sequences in exon 5, far downsteam of the polyadenylation sequence, and leading to predicted non-sense mediated decay. (E&F) Comparison of altered splicing of this exon in primary aortic endothelial cells from control and Ptbp1 EC-KO mice to alterations in low flow carotid intima, with and without platelet depletion. The percent of reads showing exon inclusion (relative to all reads from exon 4) is shown, along with the detected level of the Ripk1 full-length transcript (TpM = transcripts/kilobase per million reads).

A. GTEx Sample Table

Group	Sex	#	Mean Age, Years (STDEV)
No Athero	Male	91	48.3 (12.1)
	Female	60	50.9 (12.8)
Athero	Male	240	56.9 (9.9)
	Female	108	55.7 (10.9)

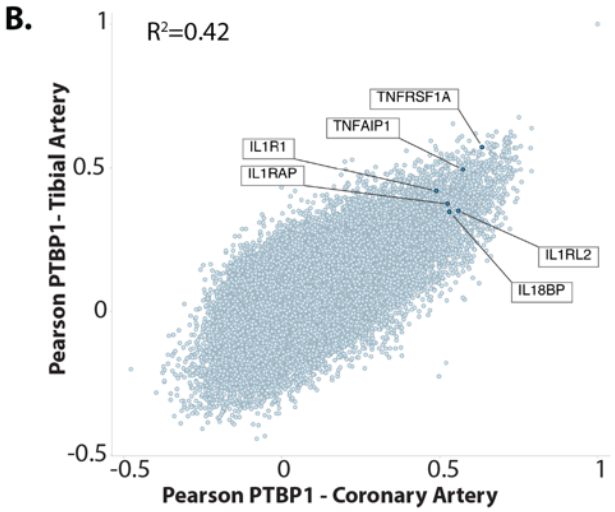

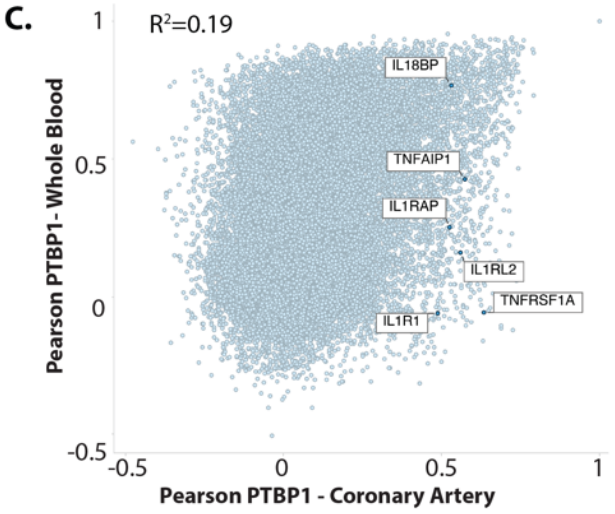

Fig. S13. Summary of GTEx samples and correlation scores between tissue types.
(A) Table shows attributes of GTEx donors for all artery samples. Generally, donors were excluded if the donor was a "biological outlier", e.g. had a large chromosomal duplication or deletion -- duplication of a whole chromosome or chromosome arm or a large CNV (>1Mb) (B&C) Gene-gene correlation plots. Correlation of each gene with the expression of PTBP1 was calculated in each sample, to give a Pearson correlation score. Graphs show the comparison of gene-specific correlation scores between tissues. For example, TNFRSF1A and IL1RL2 are strongly correlated with PTBP1 in both artery samples, but weakly correlated with PTBP1 in the whole blood samples. (B&C, GTEx v7, N=182 coronary artery samples; N=465 tibial artery samples; N=704 blood samples).

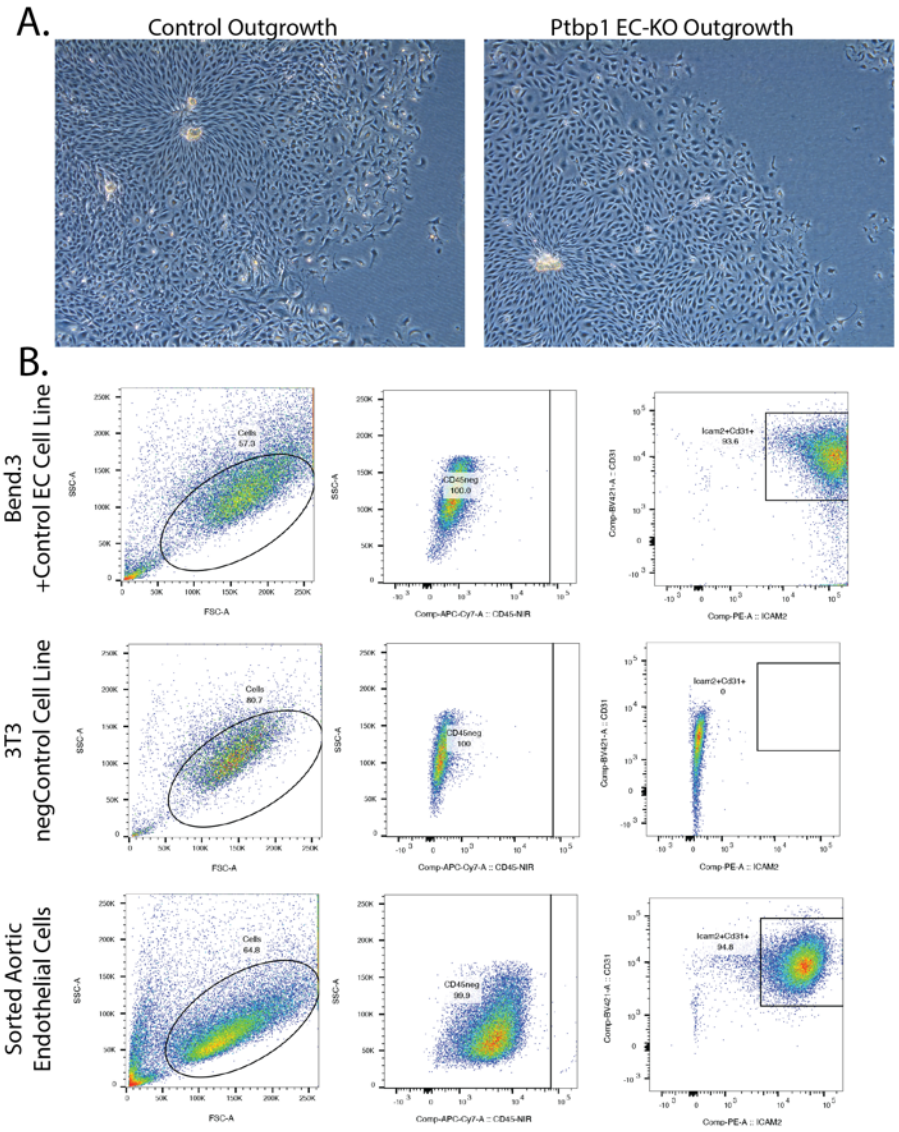

Fig. S14. Outgrowth and isolation of primary aortic endothelial cells.
(A) Images of outgrowth of primary aortic endothelial cells from collagenase flush of arterial intima. (B) Example flow cytometry plots showing positive control (Bend.3 endothelial cell line), negative control (3T3 fibroblasts) and primary aortic endothelial cells.

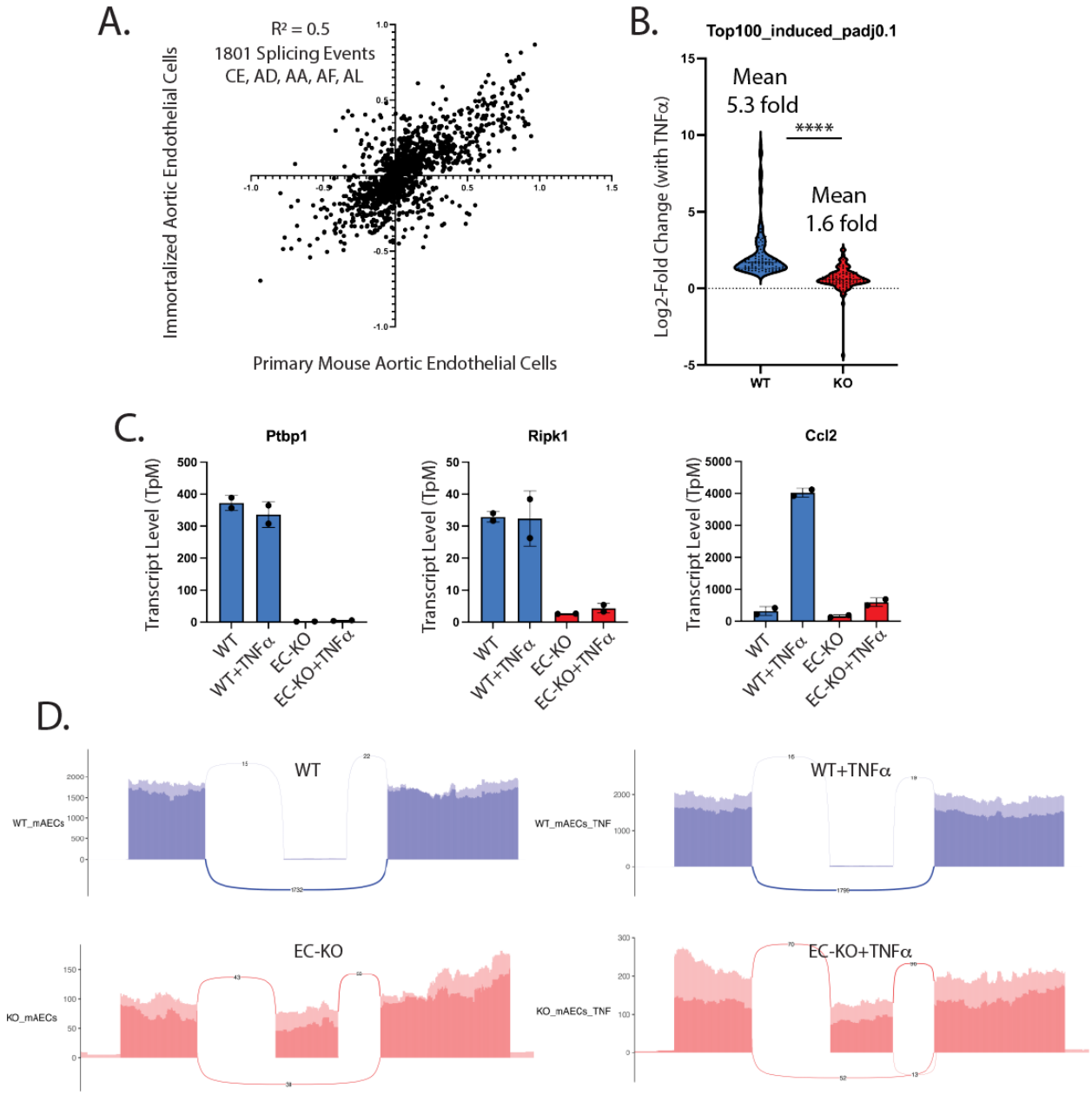

Fig. S15. Analysis of transcriptional changes in primary Ptbp1 EC-KO aortic endothelial cells
(A) Correlation plot of the effects of Ptbp1 deletion on alternative splicing events, comparing primary mouse aortic endothelial cells (dPsi between control and Ptbp1 EC-KO) to cell line (dPsi between wild-type and Ptbp1 CRISPR KO clone). CE=cassette exon, AD=alternative donor, AA=alternative acceptor, AF=alternative first, AL=alternative last. Events with probability of >0.9 in each are shown. (B) Analysis of the top 200 TNF induced transcripts (24hrs 30ng/mL TNFa), comparing the response of these transcripts in Ptbp1 EC-KO primary aortic endothelial cells to littermate controls. Axis is log2 fold-change, and actual fold change is shown on the plot. (C) Plots of transcript expression levels. TpM = transcripts/kilobase per million. (D) Sashimi plots showing inclusion levels of a Ptbp1 suppressed exon in Ripk1. Data in all plots is from two primary aortic endothelial cell (one male, one female) from each of the two genotypes (Ptbp1 EC-KO and littermate controls), and with and without TNFa treatment.

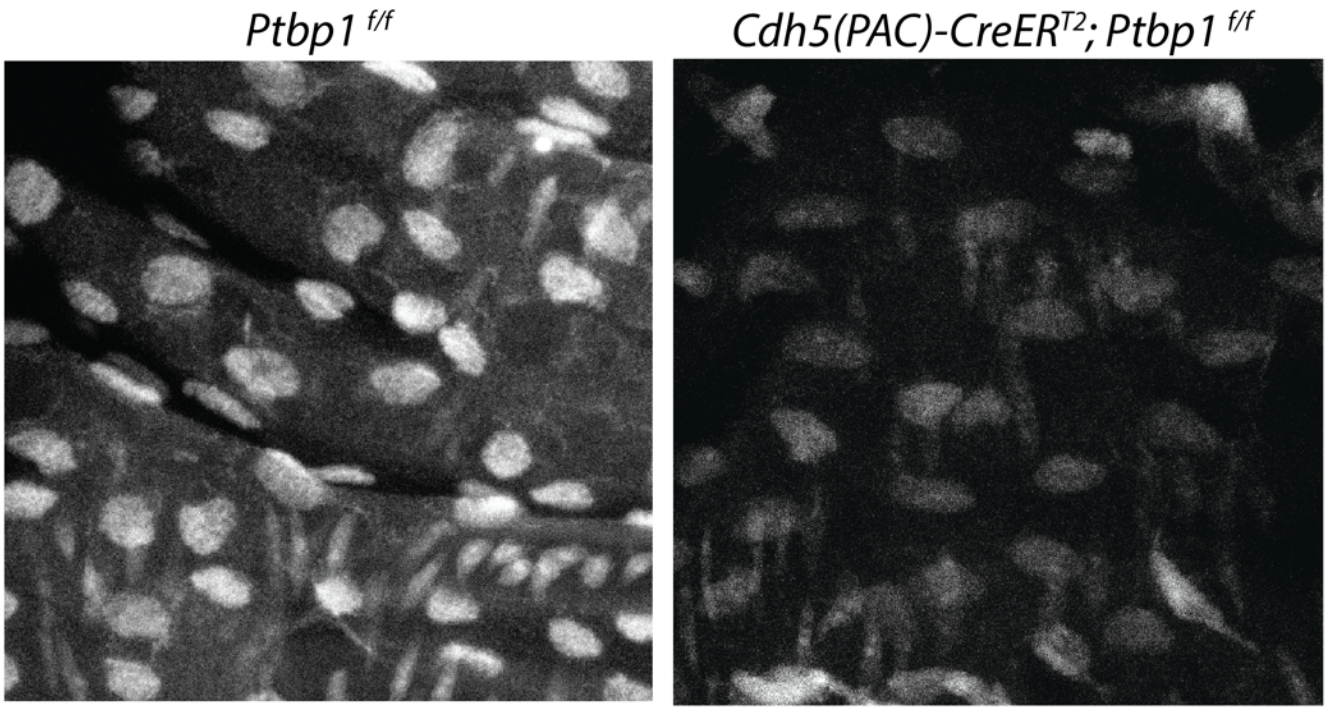

Fig. S16. En face staining of Ptbp1 in EC-KO and control mice.
Confocal imaging of Ptbp1 expression of *en face* aorta of Ptbp1 EC-KO mice and littermate controls after 3x 1mg TAM treatment.

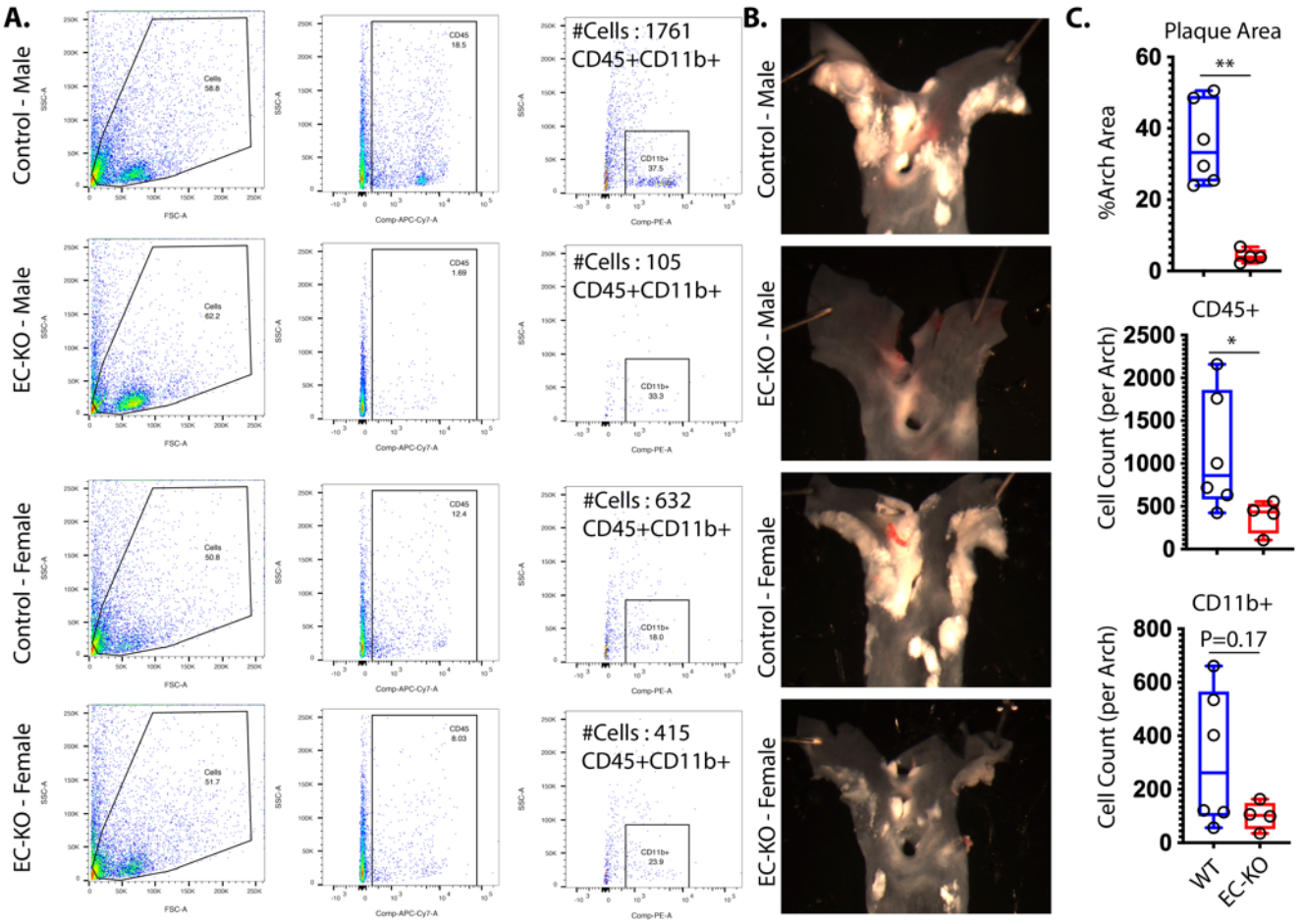

Fig. S17. Development of plaque and immune cell content in aortic arch after 5 months of hyperlipidemia. (A) Flow cytometry plots showing the analysis of CD45+CD11b+ immune cells from the aortic arches to the right. Additional mice were also processed and not shown here, but are included in the graphs to the right. (B) En face imaging of the aortic arch of these mice, showing plaque deposition. (C) Quantitation of plaque area and immune cell counts.

Fig. S18A. Analysis of innominate artery plaque.
Sequential sections (H&E stained) of innominate artery plaque, with asterisks indicating sections in which plaque inside the inner elastic lamina was quantified. Lower images show Mac3 immunostaining of the same sample (red = Mac3, blue = DAPI). Animal genotype and sex is indicated at the top.

Fig. S18B. Analysis of innominate artery plaque.
Sequential sections (H&E stained) of innominate artery plaque, with asterisks indicating sections in which plaque inside the inner elastic lamina was quantified. Lower images show Mac3 immunostaining of the same sample. Animal genotype and sex is indicated at the top. (red = Mac3, blue = DAPI)

Dataset S1.

Showing read counts per gRNA from CRISPR KO screens in murine aortic endothelial cells

Tab1 - NFkB_reporter
Sorting based on eGFP reporter of NFkB, after TNFalpha treatment.

MusAEC_NFkBrep_7days_1 (early timepoint after infection, rep 1)
MusAEC_NFkBrep_7days_2 (early timepoint after infection, rep 2)
MusAEC_NFkBrep_All_1 (all cells at time of sort, rep 1)
MusAEC_NFkBrep_All_2 (all cells at time of sort, rep 2)
MusAEC_NFkBrep_High_1 (eGFP high at time of sort, rep 1)
MusAEC_NFkBrep_High_2 (eGFP high at time of sort, rep 2)
MusAEC_NFkBrep_Mid (eGFP mid at time of sort)
MusAEC_NFkBrep_Low_1 (eGFP low at time of sort, rep 1)
MusAEC_NFkBrep_Low_2 (eGFP low at time of sort, rep 2)
Background (no cell input – testing for background in prep)

Tab2 - Icam_Vcam_Screen1
Sorting based on Icam and Vcam expression, after TNFalpha treatment.

Plasmid (plasmid library)
Splice_3day_rep_1 (early timepoint after infection, rep 1)
Splice_3_day_rep_2
Splice_3_day_rep_3
Splice_all_rep_1 (all cells at time of sort, rep 1)
Splice_all_rep_2
Splice_all_rep_3
Splice_all_rep_4
Splice_All_rep_5
Splice_Low_1 (Icam1/Vcam low at time of sort, rep 1)
Splice_Low_2
Splice_low_rep_3
splice_low_rep_4
Splice_low_rep_5
Splice_High_1 (Icam1/Vcam high at time of sort, rep 1)
Splice_High_2
Splice_high_rep_3
splice_high_rep_4
Splice_high_rep_5

Tab3 - Icam_Vcam_Screen2
Sorting based on Icam and Vcam expression, after TNFalpha treatment.
MusAEC_IcamVcam_7days_1 (early timepoint after infection, rep 1)
MusAEC_IcamVcam_7days_2
MusAEC_IcamVcam_All_1 (all cells at time of sort, rep 1)
MusAEC_IcamVcam_All_2
MusAEC_IcamVcam_High_1 (Icam1/Vcam high at time of sort, rep 1)
MusAEC_IcamVcam_High_2
MusAEC_IcamVcam_Low_1 (Icam1/Vcam low at time of sort, rep 1)
MusAEC_IcamVcam_Low_2
Background

Tab4 - Icam_Vcam_Screen3_resorted
Previous high and low samples, resorted after TNFalpha treatment.

Low_low_1
(Icam1/Vcam low in first sort, and after replating and second TNF, low again)
Low_low_2

High_high_1
(Icam1/Vcam high in first sort, and after replating and second TNF, high again)
High_high_2

Dataset S2.

Showing read counts per gRNA in samples taken early in outgrowth in murine aortic endothelial cells (3 days) and late in outgrowth (2 week and 3 week)

Dataset S3.

Showing top differential genes between clusters (EC5 vs EC4, and EC7 vs EC6), by Wilcoxon-rank test. Also showing gene set enrichment (Kegg, Hallmark, Reactome) among the top 200 genes most enriched in EC5 vs EC4 and EC7 vs EC6.

Dataset S4.

Showing results of Whippet analysis of transcript expression levels (TpM, transcripts per million).

Tab1
All data

Gene
Ensembl_ID
GeneName
TpM_May2021.PE.Cells.basal.gene.tpm (murine aortic endothelial cells, no virus)
Read_Counts_May2021.PE.Cells.basal.gene.tpm
TpM_May2021.PE.Cells.basal.TNF.gene.tpm (no virus, but with TNFalpha)
Read_Counts_May2021.PE.Cells.basal.TNF.gene.tpm
TpM_May2021.PE.Cells.KO.gene.tpm (PTBP1 CRISPR KO clone)
Read_Counts_May2021.PE.Cells.KO.gene.tpm
TpM_May2021.PE.Cells.KO.TNF.gene.tpm (PTBP1 CRISPR KO, but with TNFalpha)
Read_Counts_May2021.PE.Cells.KO.TNF.gene.tpm
TpM_May2021.PE.Cells.Rescue.gene.tpm (cDNA rescue of PTBP1 in KO)
Read_Counts_May2021.PE.Cells.Rescue.gene.tpm
TpM_May2021.PE.Cells.Rescue.TNF.gene.tpm (Rescue, but with TNFalpha)
Read_Counts_May2021.PE.Cells.Rescue.TNF.gene.tpm

Tab2 - TopUpreg
Top upregulated genes after TNFalpha treatment

Tab3 - NFkB_pathway
Canonical NFkB pathway genes

Tab4 – Inflammatory_response
Key genes involved in immune cell recruitment

Tab5 – Diff_spliced_genes
Select examples of differentially spliced transcripts and their expression levels

Dataset S5.

Showing results of Whippet analysis of differential splicing (DeltaPsi), based on percent spliced in (Psi, which is a ratio from 0-"not spliced in" to 1-"fully spliced in) with supporting read counts (Total_Reads) and Probability (statistical confidence in the difference)

Tab1 – PlateletRegulatedUnderLDF

Genes with differential regulation under disturbed flow, in a platelet dependent manner. Data from Murphy et al. eLife 2018 was re-analyzed by Whippet. Data re-analyzed from that paper is in red, new data from analysis of splicing in cultered cells +/- Ptbp1 deletion is in black. Blue is differential analysis.

Gene
Node
Coord
Strand
Type
Psi_150bp_PE_antiGr1_lig_1_expression.psi
Total_Reads_150bp_PE_antiGr1_lig_1_expression.psi
Psi_150bp_PE_antiGr1_lig_2_expression.psi
Total_Reads_150bp_PE_antiGr1_lig_2_expression.psi
Psi_150bp_PE_antiPlatelet_lig_1_expression.psi
Total_Reads_150bp_PE_antiPlatelet_lig_1_expression.psi
Psi_150bp_PE_antiPlatelet_lig_2_expression.psi
Total_Reads_150bp_PE_antiPlatelet_lig_2_expression.psi
Psi_150bp_PE_Clod_lig_1_expression.psi
Total_Reads_150bp_PE_Clod_lig_1_expression.psi
Psi_150bp_PE_Clod_lig_2_expression.psi
Total_Reads_150bp_PE_Clod_lig_2_expression.psi
Psi_150bp_PE_IgG_contra_1_expression.psi
Total_Reads_150bp_PE_IgG_contra_1_expression.psi
Psi_150bp_PE_IgG_contra_2_expression.psi
Total_Reads_150bp_PE_IgG_contra_2_expression.psi
Psi_150bp_PE_IgG_lig_1_expression.psi
Total_Reads_150bp_PE_IgG_lig_1_expression.psi
Psi_150bp_PE_IgG_lig_2_expression.psi
Total_Reads_150bp_PE_IgG_lig_2_expression.psi
Psi_150bp_PE_invitro_DMEM_expression.psi
Total_Reads_150bp_PE_invitro_DMEM_expression.psi
Psi_150bp_PE_invitro_mac_plat_expression.psi
Total_Reads_150bp_PE_invitro_mac_plat_expression.psi
Psi_150bp_PE_invitro_plasma_expression.psi
Total_Reads_150bp_PE_invitro_plasma_expression.psi
Psi_150bp_PE_invitro_plasma_mac_plat_expression.psi
Total_Reads_150bp_PE_invitro_plasma_mac_plat_expression.psi
Psi_150bp_PE_PBS_contra_1_expression.psi
Total_Reads_150bp_PE_PBS_contra_1_expression.psi
Psi_150bp_PE_PBS_contra_2_expression.psi
Total_Reads_150bp_PE_PBS_contra_2_expression.psi
Psi_150bp_PE_PBS_lig_1_expression.psi
Total_Reads_150bp_PE_PBS_lig_1_expression.psi
Psi_150bp_PE_PBS_lig_2_expression.psi
Total_Reads_150bp_PE_PBS_lig_2_expression.psi
Psi_May2021_PE_Cells_basal_TNF.psi
Total_Reads_May2021_PE_Cells_basal_TNF.psi
Psi_May2021_PE_Cells_basal.psi
Total_Reads_May2021_PE_Cells_basal.psi
Psi_May2021_PE_Cells_KO_TNF.psi
Total_Reads_May2021_PE_Cells_KO_TNF.psi
Psi_May2021_PE_Cells_KO.psi
Total_Reads_May2021_PE_Cells_KO.psi
Psi_May2021_PE_Cells_Rescue_TNF.psi
Total_Reads_May2021_PE_Cells_Rescue_TNF.psi
Psi_May2021_PE_Cells_Rescue.psi
Total_Reads_May2021_PE_Cells_Rescue.psi
DeltaPsi_PE_May2021_KO_v_Basal_TNF.diff
Probability_PE_May2021_KO_v_Basal_TNF.diff

DeltaPsi_PE_May2021_KO_v_Rescue_TNF.diff
Probability_PE_May2021_KO_v_Rescue_TNF.diff
DeltaPsi_150bp_antiPlat_v_IgG_lowflow.diff
Probability_150bp_antiPlat_v_IgG_lowflow.diff
DeltaPsi_150bp_IgG_highflow_v_IgG_lowflow.diff
Probability_150bp_IgG_highflow_v_IgG_lowflow.diff
DeltaPsi_150bp_PBS_highflow_v_PBS_lowflow.diff
Probability_150bp_PBS_highflow_v_PBS_lowflow.diff
DeltaPsi_150bp_Plasma_v_PlasmaPlateletMonocytes.diff
Probability_150bp_Plasma_v_PlasmaPlateletMonocytes.diff
DeltaPsi_150bp_Plasma_v_PlateletMonocytes.diff
Probability_150bp_Plasma_v_PlateletMonocytes.diff
EnsembleID
Gene name
BinBySpecificLimits([DeltaPsi_150bp_antiPlat_v_IgG_lowflow.diff],-0.5,-0.2,0.2,0.5)
Lists Tag Collection

Tab2 – Ptbp1RegulatedTNF
Subset showing differential splicing in aortic endothelial cell line with and without deletion of Ptbp1 (CRISPR KO), or rescue with PTBP1 cDNA.

Tab3 – Ptbp1RegulatedTNF
Subset showing differential splicing in aortic endothelial cell line with and without deletion of Ptbp1 (CRISPR KO), or rescue with PTBP1 cDNA, and in vivo with and without depletion of platelets.

Tab4 – Ptbp1_Reg_NFkB_Pathway
Subset of genes with Ptbp1 regulated splicing in the canonical NFkB signaling pathway or reactome (PMC3293857).

Tab5 – Ptbp1_Reg_NFkB_Pathway
Subset of genes with Ptbp1 regulated splicing in the canonical NFkB signaling pathway (KEGG_NFkB_hsa04064).

Dataset S6.

Showing results of corr function in GTEx (v7) data, correlating expression of Ptbp1 (TpM) with all other transcripts (TpM).

Pearson_Coronary_GeneTPM (correlation in all coronary artery samples)
Pearson_Tibial_GeneTPM (correlation in all tibial artery samples)
Pearson_WholeBlood_GeneTPM (correlation in all whole blood samples)
Pearson_Fibroblast_GeneTPM (correlation in all fibroblast samples)
Pearson_EBVlymphocytes_GeneTPM (correlation in all EBV transformed lymphocyte samples)

Dataset S7.

Showing primers used.